LEGIBILITY NOTICE

A major purpose of the Technical Information Center is to provide the broadest dissemination possible of information contained in DOE's Research and Development Reports to business, industry, the academic community, and federal, state and local governments.

Although a small portion of this report is not reproducible, it is being made available to expedite the availability of information on the research discussed herein.

1

LA-UR -86-3493

CONF-870219--1

Received by OSTI

NOV 0 1986

Los Alamos National Laboratory is operated by the University of California for the United States Department of Energy under contract W-7405-ENG-36

LA-UR--86-3493

DE87 001961

TITLE: A PORTABLE X-RAY SPECTROMETER/DOSEMETER BASED ON A SILICON DIODE

AUTHOR(S): Y. Eisen, R. H. Olsher, R. J. Brake, G. J. Littlejohn, A. Meddles

SUBMITTED TO: Health Physics Society, Reno, NV, Feb. 8-12, 1987

DISCLAIMER

This report was prepared as an account of work sponsored by an agency of the United States Government. Neither the United States Government nor any agency thereof, nor any of their employees, makes any warranty, express or implied, or assumes any legal liability or responsibility for the accuracy, completeness, or usefulness of any information, apparatus, product, or process disclosed, or represents that its use would not infringe privately owned rights. Reference herein to any specific commercial product, process, or service by trade name, trademark, manufacturer, or otherwise does not necessarily constitute or imply its endorsement, recommendation, or favoring by the United States Government or any agency thereof. The views and opinions of authors expressed herein do not necessarily state or reflect those of the United States Government or any agency thereof.

MASTER

By acceptance of this article, the publisher recognizes that the U.S. Government retains a nonexclusive, royalty-free license to publish or reproduce the published form of this contribution, or to allow others to do so, for U.S. Government purposes.

The Los Alamos National Laboratory requests that the publisher identify this article as work performed under the auspices of the U.S. Department of Energy

DISTRIBUTION OF THIS DOCUMENT IS UNLIMITED

Los Alamos

Los Alamos National Laboratory
Los Alamos, New Mexico 87545

FORM NO. 836 R4
ST. NO. 2629 5/81

A PORTABLE X-RAY SPECTROMETER/DOSEMETER BASED ON A SILICON DIODE

Y. Eisen*, R. H. Olsher, R. J. Brake, G. J. Littlejohn and A. Meddles
Mail Stop K483, Los Alamos National Laboratory,
Los Alamos, NM 87545

*Permanent Address: Soreq Nuclear Research Center, Yavne 70600, Israel

ABSTRACT

We developed a portable x-ray spectrometer/dosemeter based on a silicon p-i-n diode. The instrument is capable of obtaining spectral information in the region from 18 keV to 150 keV and measuring photon exposures in the region from 18 keV to 1.3 MeV. A theoretical method is described for obtaining a nearly air equivalent response in the energy region above 18 keV. The instrument has a dynamic range for most energies between 0.5 mR/h and 5 R/h. Its small size, ability to provide spectroscopic output, and satisfactory air equivalent response over a wide energy range, make this instrument more attractive than portable ionization chambers

INTRODUCTION

Survey meters based on ionization chambers are capable of measuring photon exposure over a wide energy range with minimal energy dependence. Providing that the chamber walls are air equivalent and charge equilibrium exists for high energy photons, such instruments have a response within $\pm$ 10% for energies above 10 keV. There are, however, several notable shortcomings for this type of instrument.

The currents measured are low; therefore, large volumes are needed. For example, for a 500 cm^3 chamber, the current is 4.6×10^{-14} Amp/mR/h. Since the chambers are usually unsealed, their response is sensitive to environmental conditions, such as pressure, temperature, and humidity. Due to their large size, they underestimate exposures from radiation leaks of small cross sectional area. And finally, ionization chambers usually operate higher than 100 volts, which complicates power supply design.

A way to overcome the need for large volume detectors is to replace air-filled ionization chambers by solid state detectors(1-4). The main disadvantage in using such detectors is that they are neither air nor tissue equivalent.

Silicon p-i-n diodes have been used in x-ray spectrometry and photon counting applications (5-7). The instrument developed in this study combines several characteristics mentioned in the above references but in addition utilizes advanced microelectronics to accurately calculate exposure rates over a wide energy range from 18 keV to 1.3 MeV.

P-i-n diodes can be operated in two modes: a pulse counting mode using a reverse bias and a current (photovoltaic) mode. In the pulse counting mode, the charge generated by the interaction is collected and is transformed to a voltage pulse. This pulse is counted if it is above the instrument's noise baseline. The pulse height is proportional to the energy deposited in the detector. In the current mode of operation, the deposited energy is converted into current. However, for low exposure rates on the order of mR/hr, the current produced is much lower than the inherent dark current of the diode. Therefore, it is necessary to use the pulse mode of operation in order to measure low-level exposures and to generate energy spectra.

The advantages of p-i-n diodes over ion chambers are as follows:

a. Only small volumes (approximately 3 mm^3) are required for measuring exposure rates on the order of 1 mR/h.

b. Diodes are relatively insensitive to environmental conditions when used in a pulse counting mode.

c. Low operating voltages (5-30 V) are sufficient.

d. Accurate measurement of exposure rates of highly localized radiation leaks are possible.

e. Diodes provide spectral information for photon energies where the photoelectric effect in silicon is still significant.

In the following we describe the theoretical basis for the algorithm used to flatten the energy response and discuss the experiments peformed to verify this algorithm. The portable dosemeter/spectrometer is then described.

THEORETICAL CONSIDERATIONS

The exposure rate, measured with an air equivalent ionization chamber, is expressed by the ionization current produced in the chamber. If the spectrum of the energy deposited in the detector, N(E), can be measured, the current flow, I, can be defined in the following way(3, 8):

$$I = k \frac{d}{dt} \int_{E_c}^{E_{max}} N(E) E \, dE \quad . \qquad (1)$$

The cutoff energy, E_c, is determined by the noise level of the detector and its associated electronics. E_{max} is the maximum energy deposited and depends on the thickness of the depletion layer, while k is a constant for matching the appropriate units.

The silicon depletion layer and its surroundings are not air equivalent. Therefore the current, I, given in Eq. 1 does not represent the exposure rate. However, if N(E) is measured, the exposure rate can be determined using a spectrum-weighting method(9) similar to those reported for NaI(Tl)(10) and for CaF_2 (Eu)(11) scintillators. Using this approach, the exposure rate, $\dot{X}$, is defined as:

$$\dot{X} = k \frac{d}{dt} \int_{E_c}^{E_{max}} \omega(E) N(E) E \, dE \quad , \qquad (2)$$

where $\omega(E)$ is the weighting function for a deposited energy E.

The integral (2) can be replaced by a discrete sum in the following way:

$$\dot{X} = k \frac{d}{dt} \sum_{i=i_0}^{i_{max}} \omega_i N_i E_i \Delta E_i \quad , \qquad (3)$$

where the index, i, refers to the energy interval between E_i and $E_i + \Delta E_i$, and ω_i and N_i are the weighting factor and the differential energy spectrum, respectively, in this energy interval.

The prime goal in this study was to find a set of weighting factors for the p-i-n diode which give best agreement with experimental results. The aim of the theoretical calculations was to find an initial set of values for ω_i to be utilized as initial parameters in an iterative least-square fitting analysis.

In the calculation of the initial set of ω_i values we took into account lost events below the cut-off energy, E_c, as well as the absorption of photons by the glass cover on the p-i-n diode. Detector resolution, escape of electrons and photons, edge effects, and lack of charge equilibrium at high photon energies were not considered in this model.

For a mono-energetic photon beam with an energy $E_{ph}>E_c$, the exposure rate $\dot{X}$ in Eq. 2 can also be expressed as:

$$\dot{X} = k \left(\frac{\mu_{en}}{\rho}\right)_{air} \Phi_{ph} E_{ph} , \qquad (4)$$

where $\left(\frac{\mu en}{\rho}\right)_{air}$ is the mass-energy absorption coefficient and Φ_{ph} is the photon flux incident on the detector. Comparing equations (3) and (4) yields:

$$\left(\frac{\mu_{en}}{\rho}\right)_{air} \Phi_{ph} E_{ph} = \frac{d}{dt} \sum_{i=0}^{i_{max}} \omega_i N_i E_i \Delta E_i . \qquad (5)$$

For photons with energies below 30 keV, the photoelectric effect in silicon is dominant and most photoelectrons are fully stopped in the detector. Thus, when $E_i \neq E_{ph}$, $\omega_i = 0$ and when $E_i = E_{ph}$,

$$\frac{dN_i}{dt} = \Phi_{ph} \left(\frac{\mu_{en}}{\rho}\right)_{Si} e^{-\mu x} \qquad (6)$$

where μ is the attenuation coefficient of the glass cover and x is its thickness. Equation (5) then yields:

$$\left(\frac{\mu_{en}}{\rho}\right)_{air} \Phi_{ph} E_{ph} = \omega_i \Phi_{ph} \left(\frac{\mu_{en}}{\rho}\right)_{Si} E_{ph} e^{-\mu x} . \qquad (7)$$

Solving for ω_i we get:

$$\omega_i = \frac{\left(\frac{\mu_{en}}{\rho}\right)_{air}}{\left(\frac{\mu_{en}}{\rho}\right)_{Si}} e^{\mu x} . \qquad (8)$$

When the photon energy is above 30 keV, the Compton effect in silicon becomes significant, and above 50 keV it dominates the total interaction cross section. Assuming that the Compton secondary photons have low interaction probability, the energy deposition spectrum has two components. The first is the total energy peak with $E \approx E_{ph}$, and the second is the Compton electron continuum whose maximum energy, T_{max}, is that of the Compton edge.

If we assume that the differential energy distribution of the Compton electrons is flat between 0 and T_{max}, that no events are present between E_{ph} and T_{max}, that photoelectrons and Compton electrons are totally

absorbed in the depletion layer, and that energy broadening can be neglected, then N_i can be expressed as follows:

$$N_i = \begin{cases} \dfrac{\sigma_{pe}}{\sigma_{total}} \dfrac{1}{\Delta E_i} & E_i = E_{ph}, \\ 0 & T_{max} \le E_i < E_{ph}, \\ \dfrac{\sigma_c}{\sigma_{total}} \dfrac{2E_{ph}}{T_{max}^2} & 0 \le E_i < T_{max}, \end{cases} \qquad (9)$$

where σ_{pe}, σ_c, and σ_{total} are the photoelectric, Compton and total absorption cross sections in silicon for photon energy E_{ph}, respectively.

The fraction, R, of the total energy deposited in the detector above the cutoff energy, $E_c < T_{max}$, is given by

$$R = \frac{\sigma_{pe} + \sigma_c\left(1 - \dfrac{E_c^2}{T_{max}^2}\right)}{\sigma_{total}} . \qquad (10)$$

For photon energies in the range 15-70 keV, the contribution to ω_i results from the full energy deposition events because the Compton events are below the cut-off energy $E_c = 15$ keV. For photon energies above 70 keV, the loss of Compton events below E_c is partial and the weighting factors are generated by both photoelectric and Compton events.

Using equations (5), (6), (9), and (10) it was possible to calculate an initial set of 11 weighting coefficients, ω_i. These coefficients were then optimized (see Results) to obtain the flattest possible energy response.

EXPERIMENTAL CONSIDERATIONS

The Detector and Electronics

We used a Hamamatsu S-1722 silicon photodiode with a sensitive area of 0.132 cm^2 and a depletion depth of 40 $\mu g/cm^2$. Glass, 1.1 mm thick, covers the front face of the diode. The detector is operated in a reverse bias mode. The noise decreases dramatically above a reverse bias voltage of 5V. We set the instrument operating voltage at 28V. As specified by the manufacturer, the maximum dark current measured at 100 V is 30 nA and the maximum junction capacity at this voltage is 12 pF.

The diode was covered with 100 $\mu g/cm^2$ of silver to make it light tight and with 0.4 mm of polyethylene to prevent contamination. It was

positioned outside an aluminum housing which contained the amplification and shaping stages. This minimizes directional dependence at low photon energies. The amplifier and shaper used with the detector was a hybrid A225 made by Amptec that has low noise characteristics. The shaped signal is further amplified by a voltage amplifier with variable gain between 10 and 100. The shaping period is 2.5 s.

The dosemeter/spectrometer includes the detector, the charge amplifications and shaping stage, and the Violinist multichannel analyzer(12).

When modified to operate in a true live time mode, the Violinist can analyze counting rates up to 3×10^4 per second with small dead time losses. At this rate the pileup probability is around 25%. The Violinist has a dot matrix LC display containing 80 x 40 cells. Three quantities are displayed: (a) The energy deposited by the secondary electrons (either the entire spectrum or only 80 channels in expand mode can be displayed). (b) The exposure rate in mR/h for three integration periods of 1, 3, or 5 seconds. (c) The accumulated exposure in mR for an arbitrary period of time. Both the exposure and the elapsed time are displayed simultaneously. The display also contains a moveable cursor. The energy corresponding to the position of the cursor and the channel number are displayed. Low battery power is indicated by a flashing display.

The gain is calibrated with an ^{241}Am source. The 60 keV peak is positioned in channel 50. In this way the instrument is able to display deposited energies up to 300 keV. Because of the small thickness of the depletion layer, only a very small number of interactions due to photons between 18 keV and 1.3 MeV, result in energy deposition above 300 keV. If events correspond to energies higher than 300 keV, they are displayed in channel 256 and are analyzed as an event corresponding to this channel.

The spectrometer/dosemeter system is operated on two 1.5 V and two 9 V batteries, and can be used continuously up to 50 hours.

Irradiations

The detector was exposed to a variety of photon sources in order to determine response characteristics such as energy resolution, energy dependence, and directional dependence. These sources consisted of fluorescent x-ray beams produced by a constant potential x-ray generator and various target materials, filtered x-ray beams, and the following radionuclides: Am-241, Co-57, Co-60, and Cs-137. The x-ray sources used are summarized in Table 1. The exposure rates were measured either with a free-air ionization chamber, Victoreen R chamber, or a Victoreen Model 440 x-ray survey meter. Exposure rates ranged from 3 mR/hr to 250 mR/hr for the x-ray sources and were as high as 170 mR/hr for the radionuclides.

Directional dependence was measured between 0° and 90° incident angle for three energies: 114 keV effective filtered beam, 76.5 keV x-ray fluorescence beam, and 43.9 keV x-ray fluorescence beam.

EXPERIMENTAL RESULTS AND DISCUSSION

Photon spectra were collected with the detector and its associated electronics at 21 photon energies between 18 keV and 1.3 MeV. The data were analyzed using a Canberra multi-channel analyzer (MCA) and a Hewlett-Packard desk-top microcomputer.

Weighting Factor Optimization

The data from the Canberra MCA were configured to simulate the operating environment of the 256 channel Violinist. All energies above 300 keV were positioned in channel 256. An initial set of 11 weighting factors corresponding to 11 energy bins in the Violinist were used to calculate an exposure in mR for each of the 21 spectra. The weighting factors were then allowed to vary over prescribed limits in a least-square fitting procedure to minimize the overall error between the reference exposure values and the calculated values. The final form of the algorithm for the exposure calculation is:

$$X(mR) = 1.72 \times 10^{-6} \sum_{i=1}^{256} \omega_i N_i E_i , \qquad (11)$$

where ω_i, E_i(keV), and N_i are the weighting factor, the energy deposited, and the number of counts, respectively, in channel i.

The optimized weighting factors are shown graphically in Figure 1. The weighting factor in the region 15-20 keV is higher than 1, compensating for the attenuation of photons by the glass cover and for lost events below the cut-off energy at 15 keV. This cut-off energy results in discriminating many events caused by Compton interactions, especially for photon energies between 50 and 150 keV. The weighting factor for deposition energies above 110 keV is greater than 1, to compensate for the lack of charge equilibrium at high photon energies and also to compensate for the Compton electrons which are discriminated by the cut-off energy at 15 keV.

Energy Resolution and Spectral Information

The energy resolution of the detector and the associated electronics was determined for two energies: at 59.6 keV using an ^{241}Am source, and at 122 keV, using a ^{57}Co source (Figure 2). The resolution was 7% and 4.5%, FWHM, respectively.

Figures 3 and 4 show several x-ray spectra obtained with the p-i-n diode. It can be seen that the detector resolution is sufficient to resolve the K_α and K_β lines of uranium with a separation energy ΔE = 15 keV as well as those of tantalum with ΔE = 9 keV. The relatively low noise permits identification of lines near 20 keV with 2.5 keV FWHM. For heavily filtered beams in which the photoelectric cross section is more than 10% of the total photon interaction cross section, a well defined peak is observed (see, for instance, the spectrum for an effective energy of 84 keV). When

the energy increases, the Compton continuum dominates the spectrum. The end-point energy of the bremsstrahlung spectra can be correlated with the peak voltage of the X-ray generator.

Directional Dependence

The directional dependence of the instrument is shown in Fig. 5 for 76.5 and 43.9 keV. It can be observed that for 43.9 keV the response at 60° is about 70% of the normal incidence response. For 114 keV effective energy, and also for the higher photon energies, the directional dependence was found to be insignificant.

Detector Efficiency and Radionuclide Identification

The intrinsic efficiency of the detector, shown in Figure 6, is defined as the ratio between the number of counts above 15 keV deposition energy and the number of incident photons impinging on the detector.

In addition to the determination of exposures, the instrument can also be used for radionuclide identification of Pu-239, Am-241, and other low-energy photon emitters in the region from 18 keV to 150 keV. Because the intrinsic efficiency of the detector at 17.6 keV is only 2.1%, the lower limit for detecting ^{239}Pu smeared uniformly on a surface will be 1 $\mu Ci/cm^2$, at contact and wit. an integration period of 3 seconds. For ^{241}Am, the intrinsic efficiency is 1.2%. Therefore, if the material is spread uniformly on a disc 6 mm in diameter, the minimum quantity to be detected in 3 seconds at a distance of 5 mm from the surface, is 3 μCi. These limits may be improved by using a p-i-n diode with a thin plastic cover.

Energy Dependence

The calculated, but unweighted exposure, is given by Equation 12:

$$X_{(mR)_{unweighted}} = 1.72 \times 10^{-6} \sum_{i=1}^{256} N_i E_i \quad . \qquad (12)$$

The uncorrected energy dependence of the dosemeter is shown in Figure 7 as the ratio of Equation 12 to the reference exposure. It can be seen that for photon energies around 40 keV the unweighted response overestimates the delivered exposure up to a factor of 4.5, whereas at high photon energies above 150 keV it is nearly equivalent to the incident exposure. This is expected from the theoretical considerations.

Figure 8 shows the corrected energy dependence of the dosemeter with the optimized weighting factors folded in. The ratio of the corrected exposure given by Equation 11 to the reference exposure is plotted as a function of photon energy.

The dosemeter overestimates the incident exposure by up to 50% for photon energies between 18 keV and 100 keV. It underestimates the exposure up to 10% above 100 keV. This response is not as good as that of an air-equivalent ionization chamber, but we feel it is satisfactory for most radiation protection purposes.

Dynamic Range

Since the number of counts per mR varies with energy, the lowest and highest exposure rates to be measured depend on the incident photon energy. The limitation at low exposure rates is counting statistics, whereas the limitation at high exposure rates is pulse pile-up and ADC dead-time in the Violinist. For common diagnostic x-ray machines, which operate at a peak voltage of 100 kV with an effective energy of about 40 keV, it is possible to measure (± 30%) an exposure rate of 0.1 mR/h for a 5 sec integration period. For an effective energy of 70 keV, the minimum exposure rate is about 0.3 mR/hr and at the highest energy of 1.3 MeV the minimum is 2 mR/h. For high counting rates, the limitation is 3×10^4 counts/sec imposed by the ADC. Pulse pile-up probability at this counting rate is about 25%. Therefore, the maximum measurable exposure rates are 1.4 R/h at 40 keV, 3.6 R/h at 70 keV, and 30 R/h at 1.3 MeV .

X-ray Machine Peak Voltage Measurement

The spectrometer/dosemeter can be used for the measurement of peak voltages of x-ray machines operating up to 200 kVp using the methodology of Nowotny (13).

A pulse pileup of 25% may lead to a 20% overestimation of end-point energies. Therefore, for peak voltage determination, we recommend that the spectrometer/dosemeter exposure rates not exceed 0.1 of the maximum exposure rates given above. As peak voltage is increased, better counting statistics are necessary to compensate for the decreasing photoelectric cross-section and the resultant poor detector efficiency.

Future Research

The energy dependence of this instrument can be improved by using very low noise p-i-n diodes and an ultra-low noise preamplifier. By lowering the noise, it will be possible to lower the cut-off energy, E_c, and measure more Compton events. It is also possible to measure photon energies below 15 keV using diodes with thin plastic covers, which are now available.

Summary

We described the development of a portable x-ray spectrometer/dosemeter using a small silicon p-i-n diode. The instrument operates at low voltages between 5 and 30 V and contains a 256 channel MCA with an 80 x 40 dot matrix LCD. The instrument provides the following capabilities:

a. Measurement of exposure rates between 0.5 mR/h and 5 R/h for photon energies in the range of 18 keV to 1.3 MeV.

b. Spectral information for photon energies between 15 and 150 keV. This spectral information permits the determination of peak voltages for x-ray machines.

c. Measurement of exposure rates from radiation leaks of small cross-sectional area.

d. The determination of the presence of low energy photon emitters such as ^{241}Am and ^{239}Pu.

The energy dependence of this instrument is not as good as that of an air equivalent ionization chamber, but is satisfactory for most radiation protection purposes.

REFERENCES

1. Huth, G. C., Recent Results Obtained with High Field Internally Amplifying Semiconductor Radiation Detectors. IEEE Trans. Nucl. Sci. NS-13 36 (1966).

2. Jones, A. R., A Portable Gamma-Ray Survey Meter using Silicon Amplifying Radiation Detectors. IEEE Trans. of Nuclear Science NS-16 (1969) 425-431.

3. Slapa, M., Belcarz, E., Chwaszezewska, J., Gruzdz, W. and Szymezyk, W., Silicon Pulse Chamber for Measurements of X and Gamma Dose Rate. Nucl. Instr. Meth. 96 239 (1971).

4. Eisen, Y., Engler, G., Ovadia, E., Shamai, Y., Baum, Z. and Levi, Y., A Small size Neutron and Gamma Dosimeter with a Single Silicon Surface Barrier Detector. 10th DOE Workshop on Personnel Neutron Dosimetry, CONF 8308140, PNL-SA-12352, September, 1983.

5. Nowotny, R. and Reiter, W. L., The Use of Silicon PIN-Photodiodes as a Low-Energy Photo Spectrometer. Nucl. Instr. Meth. 147 477 (1977).

6. Nowotny, R. and Reiter, W. L., A Comparison of Commercial p-i-n Photodiodes for X-ray Spectrometry. Nucl. Instr. Meth. 153 597 (1978).

7. Nowotny, R., A Silicon-Diode Pocket Radiation Chirper. Health Phys. 44 158 (1983).

8. Moniuchi, S. and Miyanaga, I., A Methods of Pulse Height Weighting Using the Discrimination Bias Modulation. Health Phys. 12 1481 (1968).

9. Hurst, G. S. and Ritchie, R. H., A Generalized Concept for Radiation Dosimetry. Health Phys. 8 117 (1962).

10. Takeuchi, S., Itch,. and Sekiguchi, A., A Scintillation Type Gamma-Ray Dosimeter with Low Neutron Sensitivity. Nucl. Instr. Meth. 73 148 (1969).

11. Evans, R. D., X-Ray and -Ray Interactions in Radiation Dosimetry, Vol. 1, Edited by F. H. Attix and W. C. Roesch, Academic Press, New York, 1968.

12. Umbarger, C. J., Wolf, M. A., Trujillo, F., Violinist: Sophisticated Pu Field Monitor. IEEE Transactions on Nuclear Science Volume NS-31.1, February 1984.

13. Nowotny, R., The Measurement of Peak Voltage of X-Ray Generators with Pin-Photodiodes. health Phys. 39 310 (1980).

TABLE 1

X-RAY ENERGIES USED FOR DOSEMETER CALIBRATION

Peak Voltage (kV)	Mode*	Target	Effective Energy (keV)
250	XRF	Zr	16.0
	XRF	Mo	17.8
	XRF	Ag	22.6
	XRF	BaS	33.0
	XRF	Gd	43.9
	XRF	Ta	58.8
	XRF	Pb	[illegible]
	XRF	Th	95.1
	XRF	U	100.0
100	HF		84.0
130	HF		108.0
130	HF		114.0
170	HF		135.0
170	HF		149.0
200	HF		162.0
200	HF		174.0
250	HF		205.0
250	HF		216.0
280	HF		244.0
290	HF		240.0

*XRF - beams produced by X-ray fluorescence

HF - Heavily filtered beams

Fig. 1 Weighting coefficients (see Eq. 11) as a function of the energy deposited in the p-i-n diode, for deriving the exposure in air.

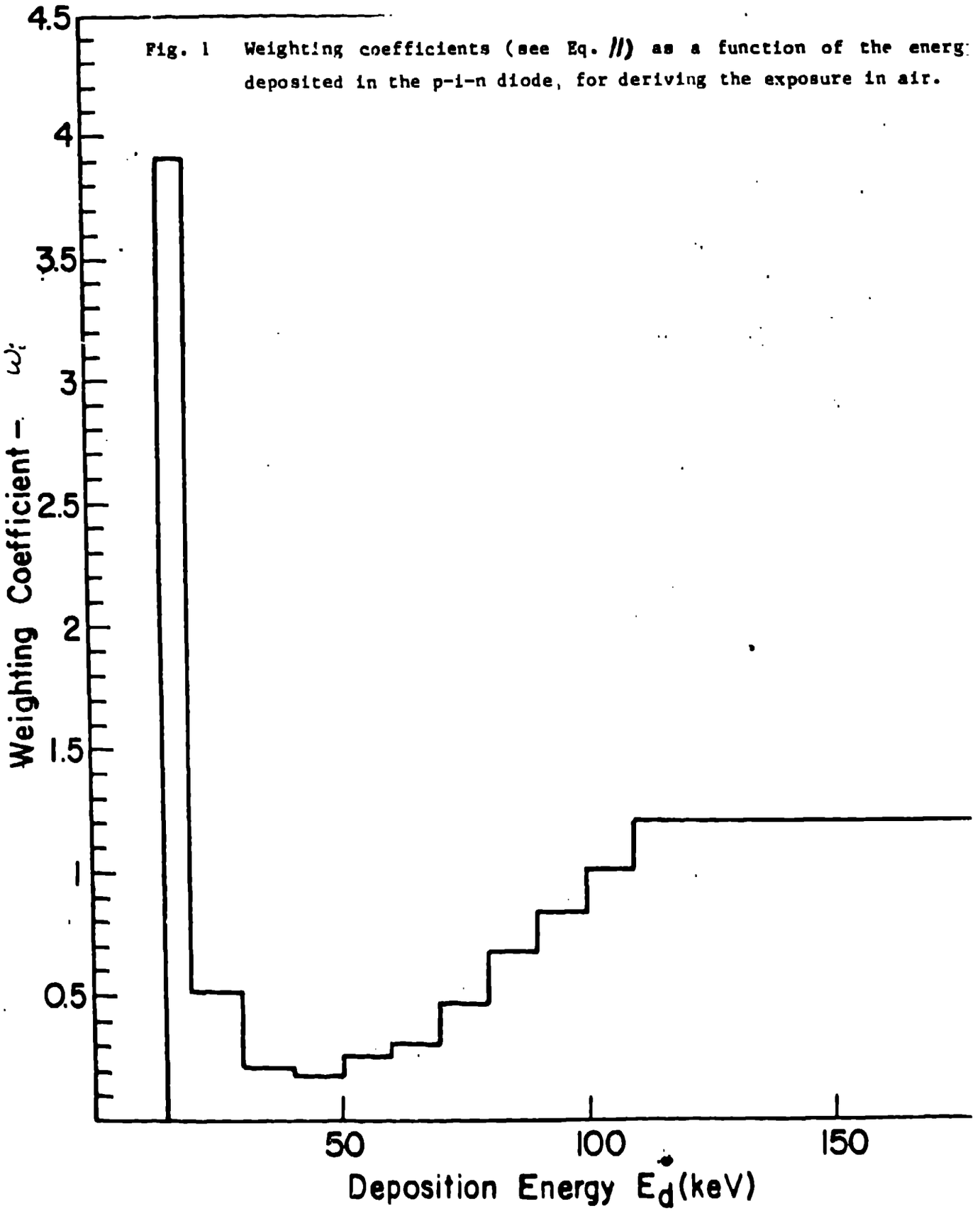

Fig. 1

Fig. 2 Energy deposition spectra obtained with the p-i-n diode for: (a) ^{241}Am (59.6 keV) and (b) ^{57}Co (122 and 136.5 keV).

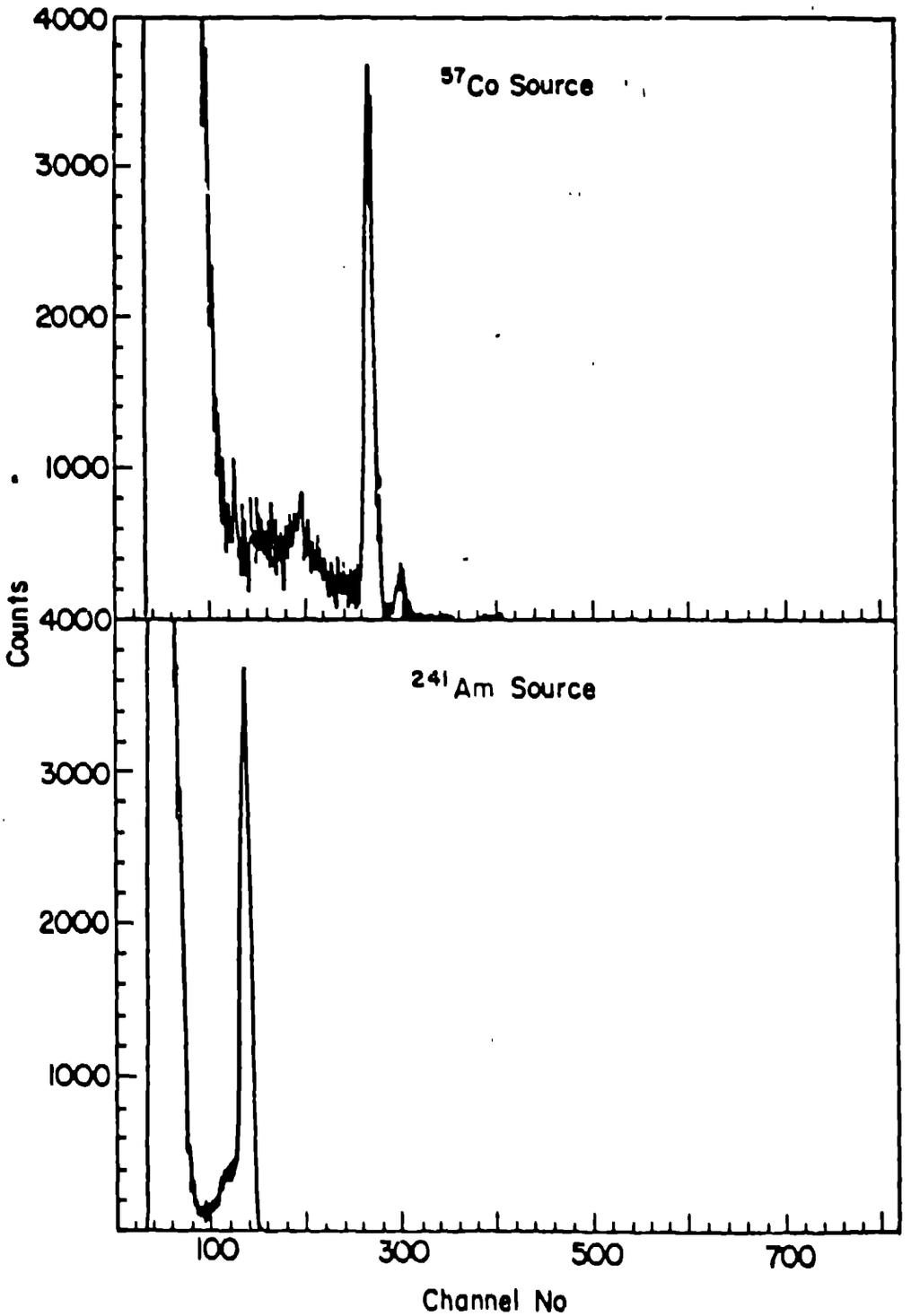

Fig 2

Fig. 3 Energy deposition spectra obtained with the p-i-n diode for X-ray fluorescence beams from Mo (17.8 keV), Ta (58.8 keV) and U (100 keV) targets.

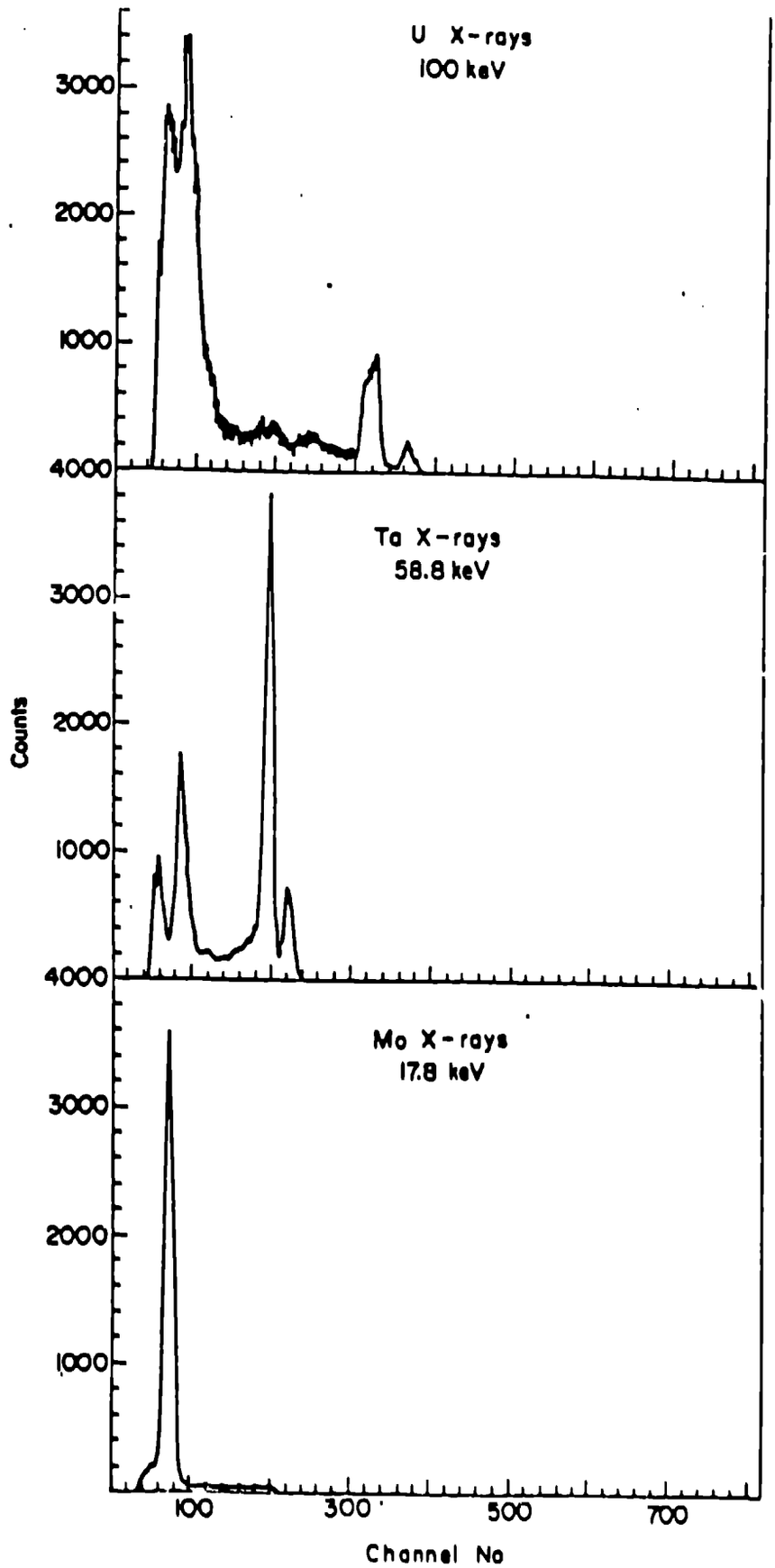

Fig. 3

Fig. 4 Energy deposition spectra obtained with the p-i-n diode for heavily filtered X-ray beams.

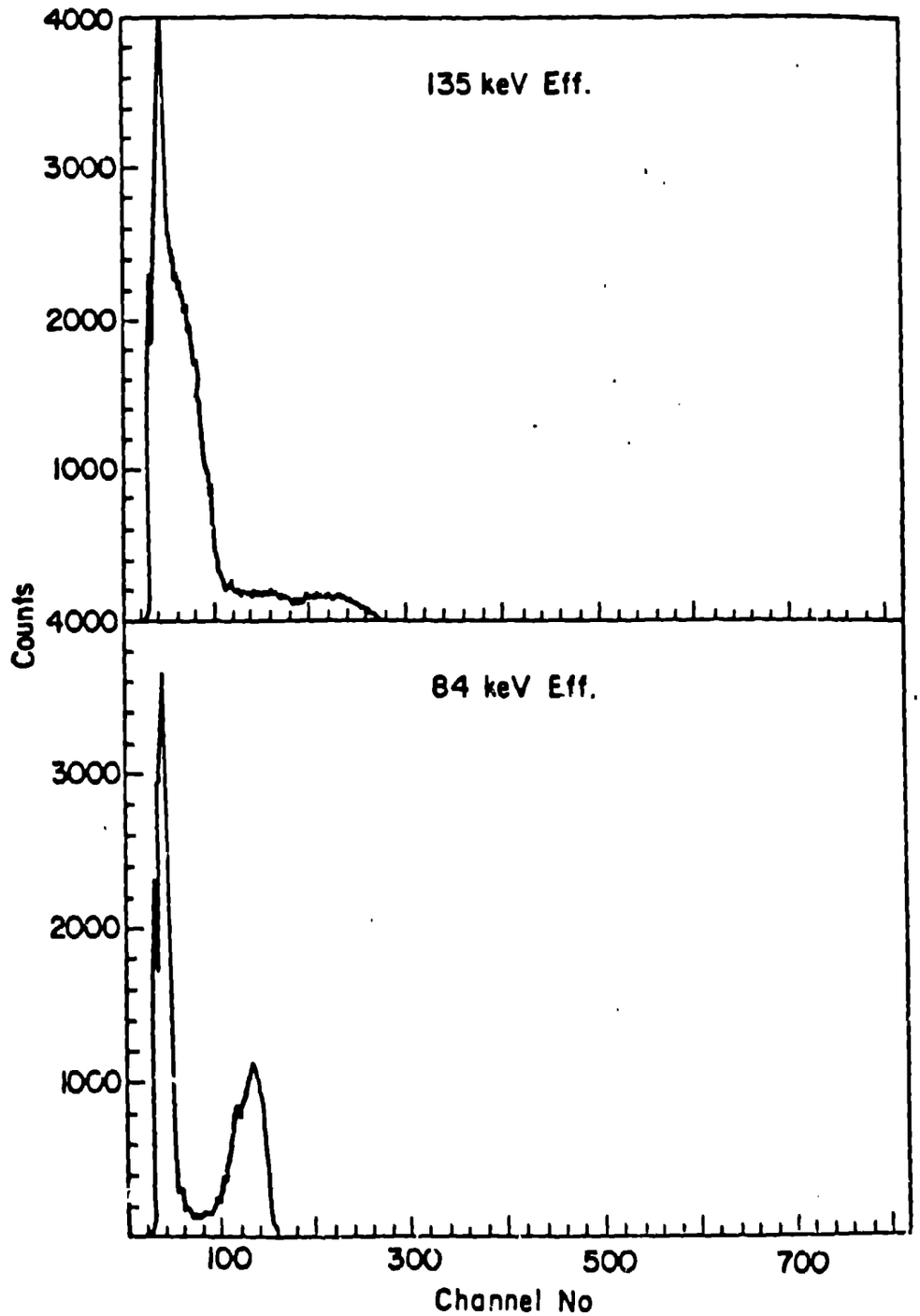

Fig 4

Fig. 5 - Directional dependence of the exposure meter for incident photon energies of 43.9 and 76.5 keV.

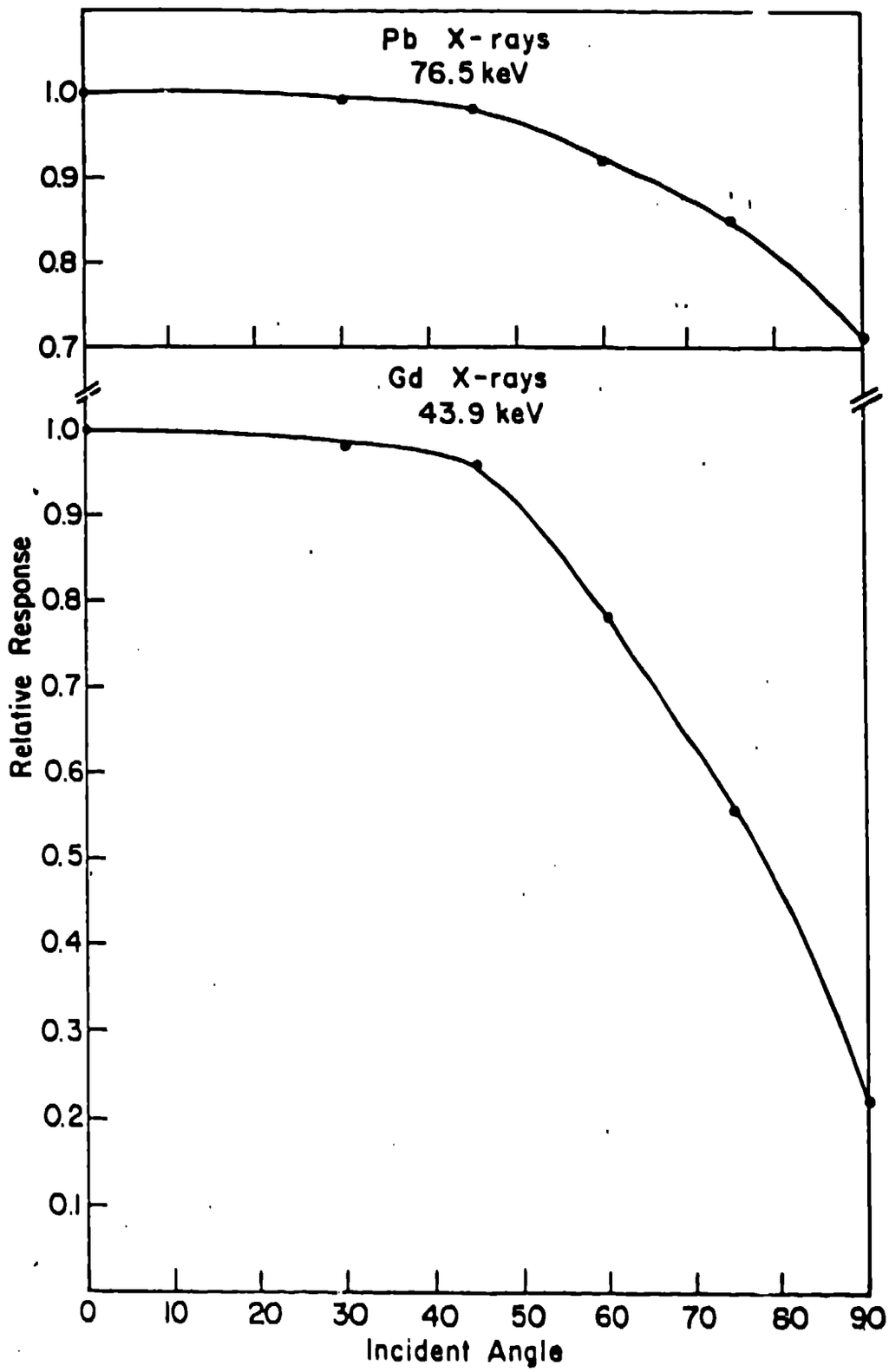

Fig. 5

Fig. 6 Intrinsic efficiency of the p-i-n exposure meter expressed as counts above 15 keV per incident photon (in percent).

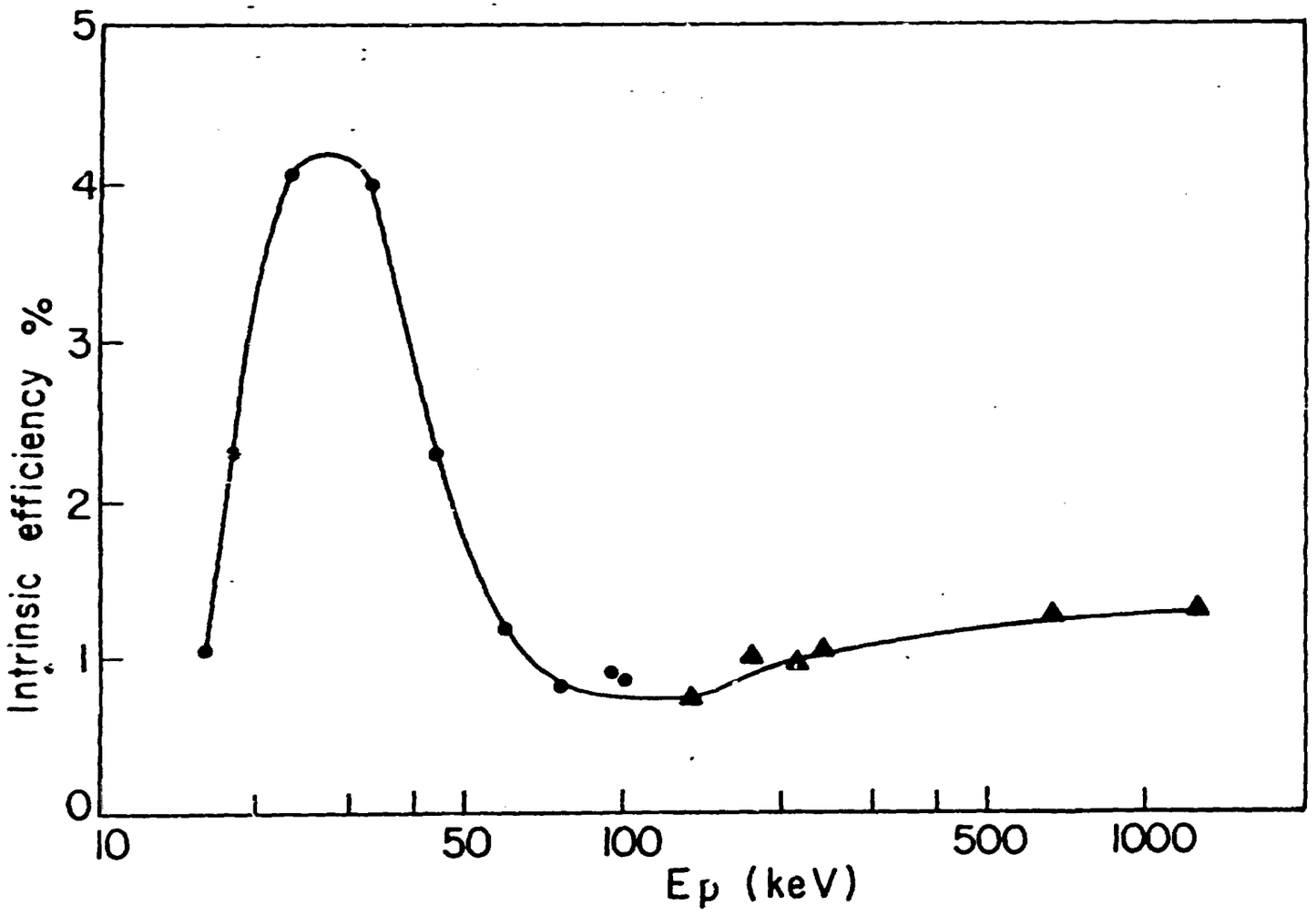

change "triangl to "dots".

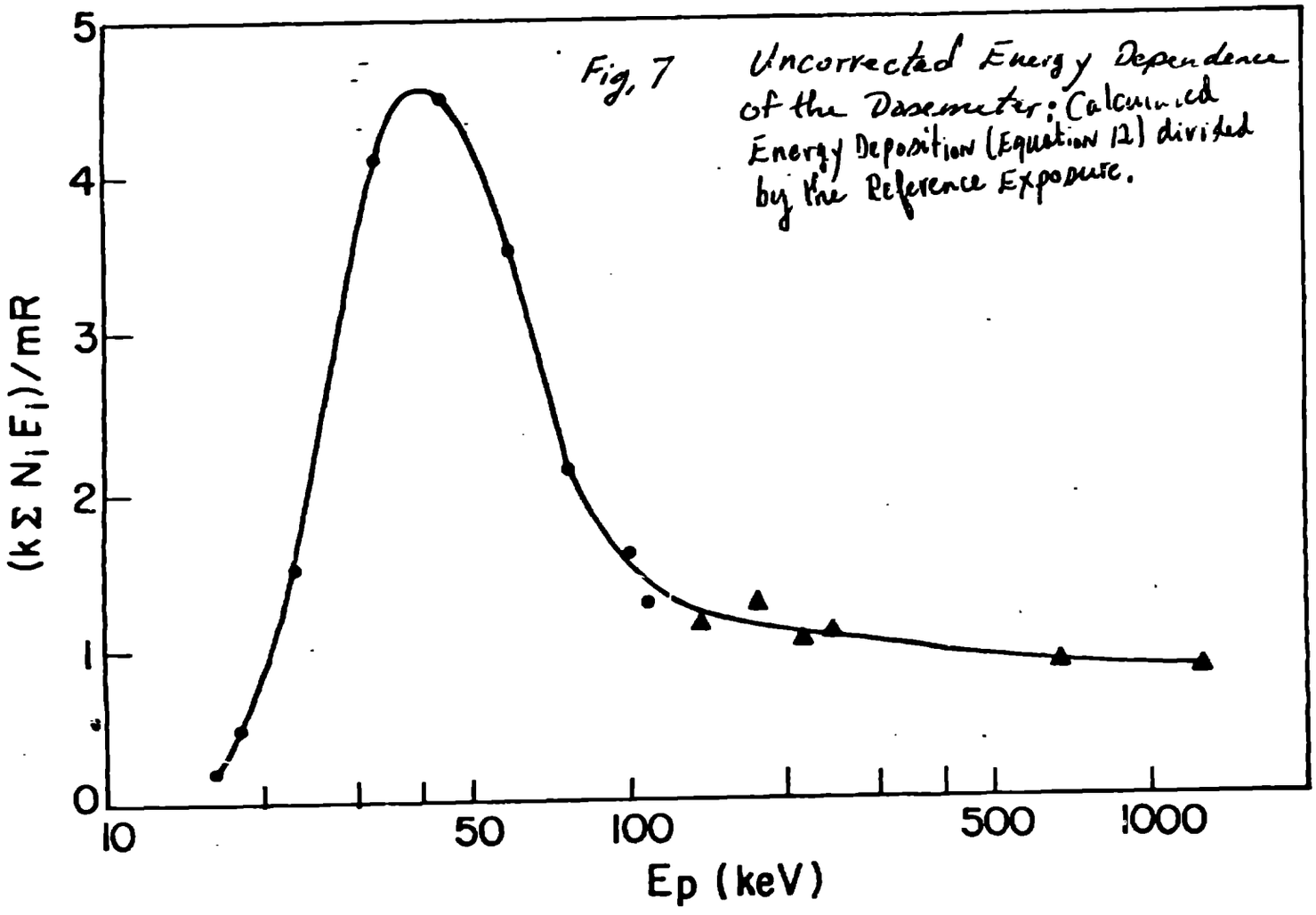

Fig. 7 Uncorrected Energy Dependence of the Dosemeter: Calculated Energy Deposition (Equation 12) divided by the Reference Exposure.

change "triangles" to "dots"

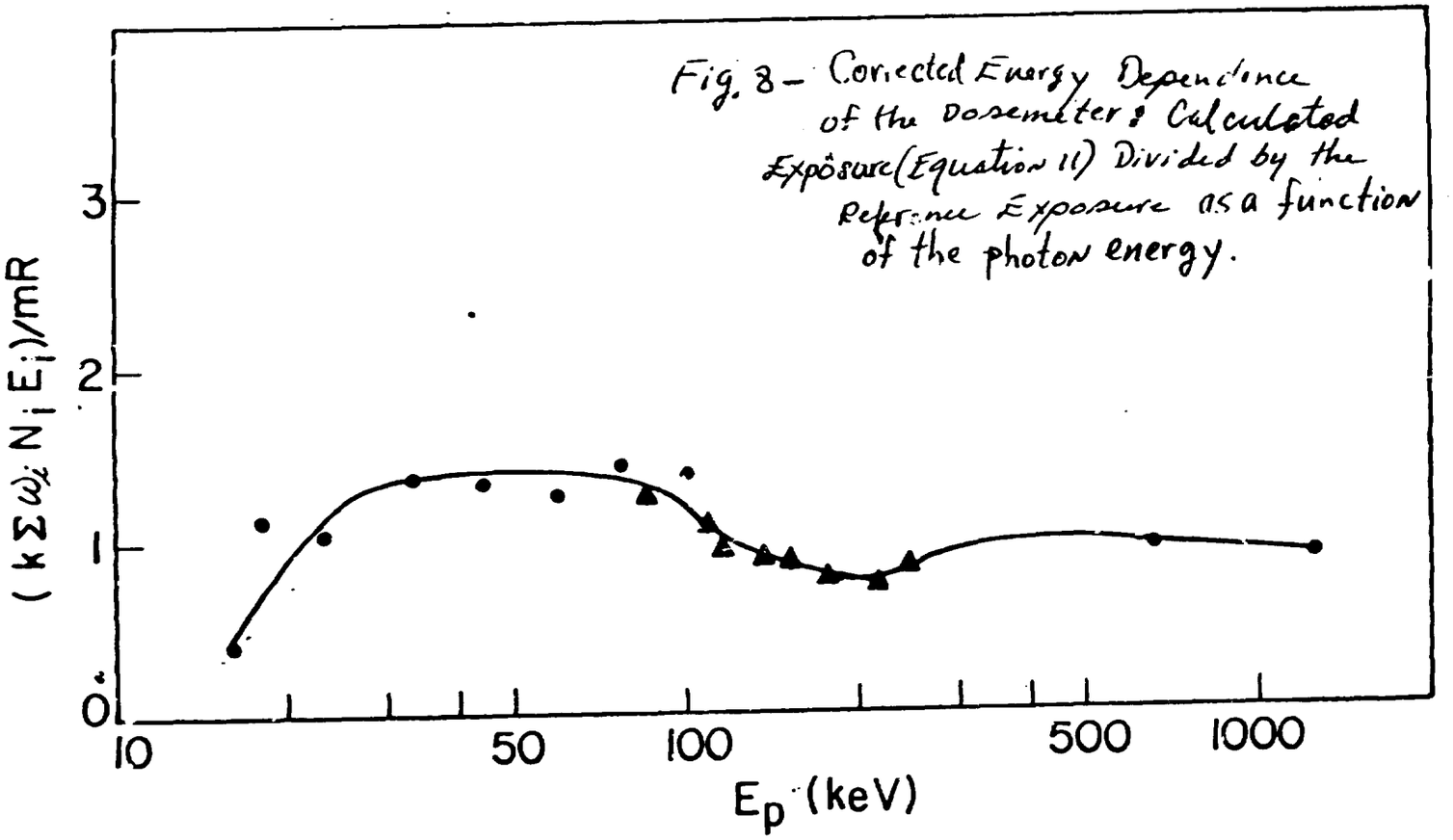

Fig. 8 – Corrected Energy Dependence of the Dosemeter's Calculated Exposure (Equation 11) Divided by the Reference Exposure as a function of the photon energy.

change "triang
to "dots"